A Model for the Propagation of Action Potentials in Nonuniform Axons

Andreas Schierwagen* and Michael Ohme†

*Institute for Computer Science, University of Leipzig, 04109 Leipzig, Germany
†Academy of Visual Arts, 04107 Leipzig, Germany

Abstract. This paper presents a method to mathematically analyze the nerve impulse propagation in nonuniform axons. Starting from the general, nonlinear one-dimensional cable equations with spatially varying cable diameter, the problem is shown to be equivalent (under some variable transformations) to the case of uniform axons. Characterized by the same normal form, six functions for analytically treatable axon diameter variations are determined. For this class of nonuniform axons, exact solutions describing the propagation of the front of the action potential are derived. The results are used to evaluate the impact of geometric non-uniformity on the properties of propagating action potentials.

Keywords: action potential, nonuniform axon geometry, nonlinear cable equation, analytical solutions
PACS: 87.10.Ca, 87.19.lb, 87.19.ll

1. INTRODUCTION

A central goal of Mathematical Neuroscience is to develop explicit mathematical models of neuronal systems that enable the explanation and prediction of systems behavior. Because of the complexity of the nervous system, mathematical modeling has been used since the early years of neuroscience to facilitate the understanding of neural functions and mechanisms.

In modeling single neurons, two types of complexity must be dealt with: the intricate interplay of active conductances underlying the complex neuronal excitation dynamics, and the elaborate dendritic morphology that allows neurons to receive and process inputs from many other neurons (e.g. [1]).

In this paper, we will discuss a method that has been used to mathematically analyze the electrical signaling function of spatially complex neurons. We will begin with presenting the model assumptions underlying the general cable model for neuronal processes. We then discuss the method used to derive analytical solutions for the electrical behavior of nonuniform neuronal segments. We then show how the results can be applied to impulse propagation in nonuniform, unmyelinated axons. Elsewhere the theory has been applied to branching dendritic trees with active membrane [2].

2. BIOLOGICAL NEURONS: MORPHOLOGY AND SIGNALING FUNCTION

The main anatomical features of neurons are as follows (Figure 1): from the cell body two kinds of processes – the dendrites and the axon – emanate. Generally, dendrites are regarded to provide receptive surfaces for input signals to the neuron. The input contacts are made by synapses which are distributed primarily over the widely branched dendritic trees. The input signals are conducted with decrement to the soma and the axon hillock. There the signals usually are converted into sequences of nerve impulses (action potentials, or spikes) which are propagated without attenuation along the axon to target cells, i. e. other neurons, muscle cells etc.

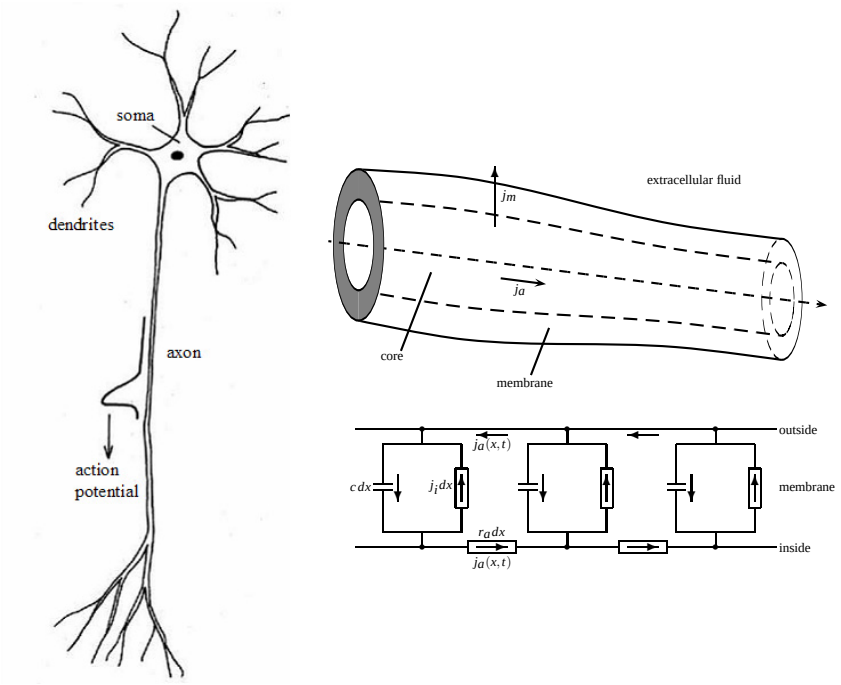

FIGURE 1. A typical textbook neuron with soma and neurites (dendrites and axon). Displayed is the current flow in a neurite segment (core conductor model) and the equivalent electrical circuit. Inside the membrane is the conducting core consisting of cell plasm, outside the extracellular fluid. In the equivalent circuit, the extracellular resistivity is neglected.

Of course, many neurons are known where this classical identification of the processing steps within a neuron must be supplemented with additional processes, such as dendritic spikes, intermittent conduction or spikeless transmission [3, 4]. Thus neurons may deviate in various ways from the above concepts which collectively comprise an idealized "standard neuron", but many of the principles seem to be common to almost all cells and probably provide the basis of neuronal operation.

The idealized neuron exhibits regionally different electrical characteristics. The soma and the dendrites have fixed ionic permeabilities, thus a change of polarization produced somewhere on the dendritic tree will spread and decay as it is conducted "electrotonically", as in a passive, leaky cable. In the axon hillock, on the other hand, the ionic

permeabilities depend on the membrane potential, and the integration of the electrotonic potentials will result in the initiation of spike trains. These two kinds of membranes are referred to as passive and active. In both cases, the spatial distribution of membrane voltage can be studied with the aid of (linear or nonlinear) cable theory.

3. GENERAL MODEL FOR NEURONAL CABLES

A model of a neuronal cable (axon or dendrite) can be set up by combining the nonlinear ordinary differential equations for an excitable membrane with the parabolic partial differential equations for a core conductor. Figure 1 schematically displays a standard neuron, the core conductor model used to represent the neurite segments and its equivalent electrical circuit. The cable equation for the transmembrane potential $V(x,t)$ and the axial current $j_a(x,t)$ is as follows (x represents distance in axial direction):

$$j_a = -\frac{1}{r_a(x)}\frac{\partial V}{\partial x}, \qquad -\frac{\partial j_a}{\partial x} = j_m = j_c + j_i \tag{1}$$

where $j_m(x,t)$ denotes the membrane current consisting of a capacitive component, j_c, and a resistive one, j_i .
We assume that the current, j_i, created by the ionic channels in the membrane can be written as a product of a resting conductance $g(x)$ which depends on the membrane surface at x , and a nonlinear voltage function $f_0(V,u_1,...,u_N)$ reflecting the threshold behavior of the voltage-dependent channels as a specific membrane property (i.e. per unit membrane surface). The latter may be time-dependent, so additional (auxiliary) variables $u_k(x,t)$ defined by first order differential equations have to be included:

$$j_c \;= c(x)\tfrac{\partial V}{\partial t}, \quad j_i = g(x)\, f_0(V,u_1,...,u_N) \tag{2}$$

$$j_m = c(x)\frac{\partial V}{\partial t} + g(x)\, f_0(V,u_1,...,u_N) \tag{3}$$

$$\frac{\partial u_k}{\partial t} = f_k(V,u_1,...,u_N) \text{ for } 1 \le k \le N. \tag{4}$$

Combining equations (1) to (3) we obtain

$$\frac{\partial}{\partial x}\left(\frac{1}{r_a(x)}\frac{\partial V}{\partial x}\right) \;=\; c(x)\frac{\partial V}{\partial t} \;+\; g(x)\, f_0(V,u_1,...,u_N). \tag{5}$$

3.1. Specific assumptions

In most cases the axial resistance $r_a(x)$ is assumed inversely proportional to the cross-section of the segment whereas the membrane conductance $g(x)$ and the membrane ca-

pacitance $c(x)$ (all quantities per unit length) are proportional to the membrane surface:

$$\begin{aligned} r_a(x) &= R_i \frac{4}{\pi d(x)^2} \\ c(x) &= C_m \pi d(x) \sqrt{1+\frac{1}{4}\left(\frac{\partial d}{\partial x}\right)^2} \\ g(x) &= G_m \pi d(x) \sqrt{1+\frac{1}{4}\left(\frac{\partial d}{\partial x}\right)^2} \end{aligned} \tag{6}$$

where $d(x)$ denotes the variable cable diameter, R_i the specific intracellular resistance, C_m and G_m the specific membrane capacitance and the resting conductance, respectively. The latter is the conductance in the nearly linear subthreshold range around the resting potential.
In the following, we will use the above equations for cables with circular cross-section. Further, we assume that $\sqrt{1+\frac{1}{4}\left(\frac{\partial d}{\partial x}\right)^2} \approx 1$, i.e. there is only weak taper, which should be satisfied in most cases. The results derived below are valid, however, also for more general *r*-, *g*-, and *c*-functions.

3.1.1. Linear cable

The simplest cable model (no auxiliary variables u_k , i.e., $N = 0$) is the linear one for passive cables. The voltage function reduces to $f_0(V) = V$ (resting potential set to zero) so the linear cable equations reduce to

$$\frac{\partial}{\partial x}\left(\frac{1}{r_a(x)}\frac{\partial V}{\partial x}\right) = c(x)\frac{\partial V}{\partial t} + g(x)V. \tag{7}$$

3.1.2. Nonlinear cable

A model of a cable with active membrane is set up by choosing suitable ionic current j_i and voltage function $\mathbf{f} = (f_1, \ldots f_N)^{\mathbf{T}}$. With such functions, system (4), (5) has been shown to simulate essential features of membrane excitation conduction. Models of increasing complexity (i.e., number of auxiliary variables) are

1. the bistable (wavefront) equation equation [5, 6] ($N = 0$)
2. the FitzHugh-Nagumo / Bonhoeffer-Van der Pol equations [7, 8] ($N = 1$)
3. the Goldstein-Rall equations [9] ($N = 2$)
4. the Hodgkin-Huxley equations [10] ($N = 3$).

Hodgkin-Huxley model. The Hodgkin and Huxley (HH) model has been used as basis of most of the conductance-based models. In the original version, the model

consists of a four-dimensional system of nonlinear differential equations [10]. The ionic current, j_i, is determined by three conductances where two of them are voltage-dependent:

$$\begin{aligned} j_i &= j_{Na} + j_K + j_L \\ &= g_{Na}(V - E_{Na}) + g_K(V - E_K) + g_L(V - E_L) \\ &= m^3 h \bar{g}_{Na}(V - E_{Na}) + n^4 \bar{g}_K(V - E_K) + g_L(V - E_L), \end{aligned} \tag{8}$$

and $\bar{g}_{Na}$, $\bar{g}_K$ are the maximal conductance values of the sodium and potassium channels, and g_l is the (constant) value of the passive leak conductance. $u_1 = m$ and $u_2 = h$ are the activation and inactivation variables for sodium, $u_3 = n$ is the activation variable for potassium,$0 < m, n, h < 1$, and the following differential equations hold

$$\begin{aligned} \frac{\partial m}{\partial t} &= f_1 \quad = \alpha_m(1-m) - \beta_m m \\ \frac{\partial n}{\partial t} &= f_2 \quad = \alpha_n(1-n) - \beta_n n \\ \frac{\partial h}{\partial t} &= f_3 \quad = \alpha_h(1-h) - \beta_h h \end{aligned} \tag{9}$$

where $\alpha_m, \beta_m, \alpha_n, \beta_n, \alpha_h, \beta_h,$ are empirical functions of the voltage V. The leak conductance $g_L(x) = G_L \pi d(x)$, according to (6). We rewrite (8) as

$$j_i = g \cdot f_0(V, m, n, h) = g(x) \left(\frac{\bar{g}_{Na}}{\bar{g}_L} m^3 h (V - E_{Na}) + \frac{\bar{g}_K}{\bar{g}_L} n^4 (V - E_K) + (V - E_L) \right). \tag{10}$$

Thus the part of the current j_i depending on cable diameter is separated from the voltage-depending part, in accordance with the general cable equation (5).

FitzHugh-Nagumo model. Below we will use the FitzHugh-Nagumo (FHN) model, a simplified version ($N = 1$) of the Hodgkin-Huxley model, to study nerve conduction. The FHN equations [7] can be written as:

$$\begin{aligned} j_m &= c(x)\frac{\partial V}{\partial t} + g f_0 = c(x)\frac{\partial V}{\partial t} + g(h(V) + u) \\ \frac{\partial u}{\partial t} &= \alpha V - \beta u \end{aligned} \tag{11}$$

with resting potential equal to zero and cubic $h(V) = V(1 - V/V_1)(1 - V/V_2)$ where $0 < V_1 < V_2$ are the roots of h . The constants α and β are positive so that u acts as a variable which takes the system from the excited state (near V_2) back to the resting state $V = 0$.

4. TRANSFORMATION INTO NORMAL FORM

We transform Eq. (5) by the variable transformation (applied already by Kelly and Ghausi [11] and later by Schierwagen [12])

$$\begin{aligned} T &= \frac{t}{\tau} \quad \text{with} \quad \tau(x) = \frac{c(x)}{g(x)} \text{ and} \\ X &= \int_0^x \frac{d\hat{x}}{\lambda(\hat{x})} \quad \text{with} \quad \lambda(x) = \frac{1}{\sqrt{r_a(x)g(x)}}. \end{aligned} \tag{12}$$

For an uniform cable (i.e. c, g and r_a independent of x), λ and τ are constant and equal to the length and time constants of passive cable theory.

Now Eqs. (4), (5) can be rewritten:

$$\begin{aligned} 0 &= \frac{\partial^2 V}{\partial X^2} + Q(X)\frac{\partial V}{\partial X} - \frac{\partial V}{\partial T} - f_0(V, u_1, ..., u_N) \\ \frac{\partial u_k}{\partial T} &= \tau(X) f_k(V, u_1, ..., u_N) \quad \text{for } 1 \le k \le N \end{aligned} \tag{13}$$

with

$$Q(X) = \frac{1}{2}\frac{\mathrm{d}}{\mathrm{d}x}\ln\left(\frac{g(X)}{r_a(X)}\right). \tag{14}$$

$Q(X)$ contains all geometry-dependent parts of the transformed cable equation and can therefore be used for classifying cable geometries. For example, in the standard case of a cable with circular cross-section, we obtain

$$Q(X) = \frac{\mathrm{d}}{\mathrm{d}x}\ln D(X)^{\frac{3}{2}}. \tag{15}$$

In particular, $Q = 0$ for cylindrical cable geometries (i.e., r_a and g are constant), whereas Q remains nearly constant for a (slowly) exponentially tapering cable diameter in Eqs. (6), positive for increasing and negative for decreasing diameter.

Using the transformations

$$\begin{aligned} V(X,T) &= F(X) \cdot W(X,T) \\ u_k(X,T) &= F(X) \cdot w_k(X,T) \end{aligned} \tag{16}$$

with

$$F(X) = \exp(-\frac{1}{2}\int Q(X)\mathrm{d}X) = D(X)^{-\frac{3}{4}}, \tag{17}$$

the equations (5) or (13), respectively, in normal form read

TABLE 1. Axon geometries as defined by the solutions of the special Riccati equation $2Q' = 4P - Q^2$. The stationary solution is denoted by $Q_1 = \pm 2\sqrt{P}$ (cf. [1]). C_1 and $C_2 > 0$ are free but constant parameters.

Geometry type	P	$Q(X)$	$\frac{g(X)}{r_a(X)} = F(X)^{-4}$
uniform	$P = 0;\ Q = 0$	0	C_2
power	$P = 0;\ Q \neq 0$	$\frac{2}{X - C_1}$	$C_2(1 - \frac{X}{C_1})$
exponential	$P > 0;\ Q^2 = Q_1^2 = 4P$	Q_1	$C_2 \exp(2Q_1 X)$
hyperbolic sine	$P > 0,\ \|Q\| > Q_1$	$Q_1 \coth(\frac{X - C_1}{2})$	$C_2(\sinh(Q_1 \frac{X - C_1}{2}))^4$
hyperbolic cosine	$P > 0;\ \|Q\| < Q_1$	$Q_1 \tanh(\frac{X - C_1}{2})$	$C_2(\cosh(Q_1 \frac{X - C_1}{2}))^4$
trigonometric cosine	$P < 0$	$-\|Q_1\| \tan(\|Q_1\| \frac{X - C_1}{2})$	$C_2(\cosh(\|Q_1\| \frac{X - C_1}{2}))^4$

$$\frac{\partial^2 W}{\partial X^2} - P(X)W - \frac{f_0(FW, Fw_1, ..., Fw_N)}{F} - \frac{\partial W}{\partial T} = 0$$
$$\frac{\partial u_k}{\partial T} = \tau \frac{f_k(FW, Fw_1, ..., Fw_N)}{F} \text{ for } 1 \leq k \leq N. \tag{18}$$

For linear functions $f_k\,(k = 0, ..N)$, the transformation function $F(X)$ cancels in the equations. This is the case for, e.g., the bistable wavefront equation or the piecewise linear FitzHugh-Nagumo equations (see below). In the following, this case is assumed to hold.

The coefficient $P(X)$ is defined by the simple Riccati equation [1, 11, 12]:

$$P(X) = \frac{1}{2}Q'(X) + \frac{1}{4}Q(X)^2. \tag{19}$$

Various classes of nonuniform cable geometries may be obtained by choosing the function $P = P(X)$ in condition (19). The simplest class to consider are those cables for which P is a constant. This class can be determined by solving the Riccati differential equation (19). The complete solution set and the corresponding diameter functions determined from (15) are given in Table 1.

5. AXON GEOMETRIES REDUCIBLE TO THE UNIFORM CASE

If we take a closer look at the function $Q(X)$ defined by Eq. (15), we can derive explicit conditions relating the diameter of the cable in the range, $D(X)$, and that of the domain, $d(x)$. For this we calculate the back transform of the solutions from Table 1 from the range into the domain. This is not trivial because of the space-dependency of λ. Table 2 shows the transforms for the space variables $X(x)$ and $x(X)$ which follow from (12) with

$$\lambda(x) = \frac{1}{\sqrt{r_a(x)g(x)}} = \frac{\lambda_0}{d_0}\sqrt{d(x)} \tag{20}$$

where $d_0 = d(0)$, $\lambda_0 = \lambda(0)$. Appropriate transformations can be given also in the case of diameter changes which are not negligible [13].

By inverting the defining equation (17) for $F(X)$ and using the Riccati equation (19), we find after some lengthy calculations

$$P(D) = \frac{\left(D(X)^{3/4}\right)''}{\left(D(X)^{3/4}\right)} \tag{21}$$

and with $\mathrm{d}x/\mathrm{d}X = 1/\lambda(x)$ (cf. Eq. (12))

$$p(d) = \frac{3}{20\,G_m R_i}\frac{\left(d(x)^{5/4}\right)''}{d(x)^{1/4}}. \tag{22}$$

For $p(d) = 0$ we can now analytically calculate the domain solutions of the image diameter functions for the uniform and power case (see Table (3)). In the other cases, an implicit equation in $d = d(x)$ can be given:

$$\pm\frac{8\sqrt{G_m R_i p}}{3}x + c_2 = \int \frac{d^{1/4}}{d^{3/4} + c_1}\mathrm{d}d \tag{23}$$

which only for $c_1 = 0$ can be solved in closed form. In this case, the domain solution of the exponential diameter function yields the quadratic geometry type (Table 3).

6. TRAVELING WAVES IN NON-UNIFORM AXONS

6.1. General model with nonuniform geometry

In most cases, theoretical investigations of spike propagation assume uniform electrical and geometric properties along the axon. From these analyses, much insight into propagation mechanisms has been gained, suggesting constant shape and velocity of the propagating spike in axons with uniform geometry. A linear or square root relationship between velocity and axonal diameter for myelinated and unmyelinated nerve fibres, respectively was deduced [14].

TABLE 2. Transforms for the space variables $X(x)$ and $x(X)$, respectively.

Geometry type	P	$X(x)$	$x(X)$
uniform	$P = 0;\ Q = 0$	$\frac{x}{\lambda_0}$	$x\lambda_0$
power	$P = 0;\ Q \neq 0$	$C(1-(1-\frac{5x}{3\lambda_0 C})^{\frac{3}{5}})$	$\frac{3}{5}C\lambda_0(1-(1-\frac{X}{C})^{\frac{5}{3}})$
exponential	$P > 0;\ Q = Q_1$	$\frac{3}{Q_1}\ln(1+\frac{Q_1}{3\lambda_0}x)$	$\frac{3}{Q_1}\lambda_0(\exp(\frac{Q_1}{3}X)-1)$

TABLE 3. Corresponding diameter functions $d(x)$ and $D(X)$ of nonuniform cable in the domain and in the range, respectively.

Geometry type	P	$D(X)$	$d(x)$
uniform	$P=0;\ Q=0$	d_0	d_0
power	$P=0;\ Q\neq 0$	$d_0(1-\frac{X}{C})^{\frac{4}{3}}$	$d_0(1-\frac{5x}{3\lambda_0 C})^{\frac{4}{5}}$
exponential	$P>0;\ Q=Q_1$	$d_0\exp(\frac{2}{3}Q_1X)$	$d_0(\frac{Q_1x}{3\lambda_0}+1)^2$

However, experimenters have noted several effects which could not be explained with this theory. Examples are blocking of impulse conduction, frequency modulation and changes of AP shape in regions of nonuniform axon geometries (for review, see [15]). Motivated by these observations, several investigators studied the effects of changing axonal geometry upon AP propagation, both by theoretical and computational methods (e.g. [16]).

A drawback of a pure computer simulation approach has been, however, the impossibility of exploring analytically how the various physical parameters describing the inhomogeneous axon affect the solution. Goldstein and Rall [9] instead used results from dimensional analysis [17] to compare theoretical axons having different values of physical parameter but identical nonlinear membrane properties. Our analysis below is inspired by this approach.

We consider traveling wave solutions of the normalized cable equations (13). Thus, we assume that in these equations only the geometry-defining parameter Q explicitly depends on the space variable X whereas all f_k are independent of X, i.e. the voltage thresholds of all channels do not vary in space. The same should hold for the auxiliary variables $u_k(X,T)$. Then we make the ansatz $W(X,T)=W(Y)$ with $Y=X-\Theta T$, which means that a fixed voltage shape travels with constant velocity Θ along the cable (for positive Θ from left to right). Now the system of ordinary differential equations to be solved reads:

$$0=\frac{\mathrm{d}^2W}{\mathrm{d}Y^2}+(\Theta+Q)\frac{\mathrm{d}W}{\mathrm{d}Y}-f_0(W,u_1,...,u_N) \tag{24}$$

$$\frac{\mathrm{d}u_k}{\mathrm{d}Y}=-\frac{\tau}{\Theta}f_k(W,u_1,...,u_N)\quad \text{for } 1\leq k\leq N. \tag{25}$$

For an uniform cylindrical cable, $Q=0$, after definition of Q in (15). Only in this case Eq. (24) remains invariant with respect to the substitution $\Theta\rightarrow-\Theta$ and $Y\rightarrow -Y$ which means that for any leftwards traveling wave with velocity Θ^-, there is also a wave traveling rightwards with velocity $\Theta^+=-\Theta^-$, and vice versa.

For $Q>0$ (the analog is true for $Q<0$) in some part of the axon cable this symmetry is broken – the range of possible wave velocities will be 'shifted'. For the general case of Eq. (24) no exact quantitative value of this shift can be given. We can explore it qualitatively, however, by looking at the velocity of the leading wave-front. Assuming that the u_k-kinetics are slower than the W-kinetics, we set $u_k=0$ during the build-up of the leading impulse front [18]. Eq. (24) then reads:

$$0 = \frac{\mathrm{d}^2 W}{\mathrm{d}Y^2} + (\Theta + Q)\frac{\mathrm{d}W}{\mathrm{d}Y} - f_0(W). \tag{26}$$

Let the uniform cable equation with $Q = 0$ admit two traveling wave fronts (an excitation from the resting potential to some excited state) at a speed of Θ_{uni}, from right to left with $\Theta^- = -\Theta_{uni}$, and from left to right with $\Theta^+ = \Theta_{uni}$. Then the nonuniform cable admits two wave solutions with the shifted propagation velocities $\Theta^- = -(\Theta_{uni} + Q)$ and $\Theta^+ = \Theta_{uni} - Q$. For cable diameters increasing sufficiently strong from left to right (high values of the geometry parameter Q) we find two wave solutions traveling to the left ($\Theta^- < \Theta^+ < 0$) but none traveling to the right. Here the leftwards traveling front has also a much higher speed than the fronts in the uniform cable. These results demonstrate the direction-dependence of the spike propagation in non-uniform cables (see below and [2, 19]).

6.2. FHN model

As stated in Section 4, for linear functions $f_k(k = 0,..N)$, the transformation function $F(X)$ cancels in the equations (18). Using the FHN model (11) with

$$f_0(W, W_1) = H(W) + W_1 \tag{27}$$

where $H(W) = \widehat{m}_i W - n_i$ represents a piecewise linear membrane characteristic (Figure 2), we get from (18)

$$\begin{aligned} \frac{\partial^2 W}{\partial X^2} - \frac{\partial W}{\partial T} - (P(X) + \widehat{m}_i)W + n_i - w = 0 \\ \frac{\partial w}{\partial T} = \tau(\alpha W - \beta w). \end{aligned} \tag{28}$$

For $P(X) = const$ the system (28) corresponds to the basic equations of uniform cable geometry, thus the results derived by others (see [20] for review) and the present authors [2, 19] can be used. The equations then read:

$$\begin{aligned} \frac{\partial^2 W}{\partial X^2} - \frac{\partial W}{\partial T} - m_i W + n_i - w = 0 \\ \frac{\partial w}{\partial T} = \tau(\alpha W - \beta w) \end{aligned} \tag{29}$$

while we set $m_i := P + \widehat{m}_i$.

For the linear regions of $H(W)$ there are traveling wave solutions. Employing the results of Section 5, the system of ordinary differential equations (24), (25) can be written as:

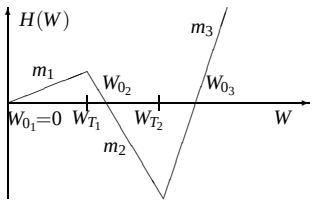

FIGURE 2. Piecewise linear approximation $H(W) = m_i W - n_i$ of the membrane current-voltage characteristic. In the general case, there are three linear regions of $H(W)$, $J_i = [W_{T_i}, W_{T_{i+1}}]$, each containg a zero.

$$\frac{\mathrm{d}^2 W}{dY^2} + \Theta \frac{\mathrm{d}W}{\mathrm{d}Y} - m_i W + n_i - w = 0$$
$$\Theta \frac{\mathrm{d}w}{\mathrm{d}Y} = -\tau(\alpha W - \beta w). \tag{30}$$

We will consider the bistable case; it is represented by $m_2 \to \infty$ where the middle zero, W_{0_2}, merges with the boundaries W_{T_1}, W_{T_2} to give a threshold, $W_T := W_{T_1} = W_{T_2} = W_{01}$ (see Figure 2).

Eq. (27) becomes

$$f_0(W) = \begin{cases} m_1 W & \text{for} \quad W < W_{0_2} \\ m_3(W - W_{0_3}) & \text{else} \end{cases} . \tag{31}$$

The simplest case to consider is $\alpha = \beta = 0$, i.e. the propagation of a wave front (Figure 3) with velocity Θ , without recovery from the excited state.

Eqs. (30) simplify to:

$$\frac{\mathrm{d}^2 W}{\mathrm{d}Y^2} + \Theta \frac{\mathrm{d}W}{\mathrm{d}Y} - m_i W = 0. \tag{32}$$

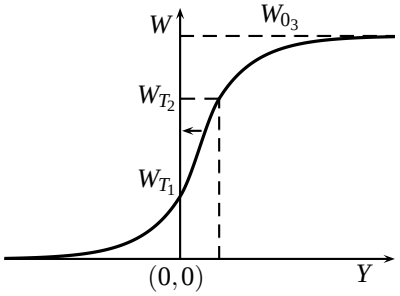

FIGURE 3. Wave front moving to the left while changing the voltage level from 0 to W_{0_3}.

The functions $W(Y)$ in the two regions separated by W_{0_2} can be specified as follows:

$$W(Y) = \begin{cases} W_{0_2} \exp(\mu_1 Y) & \text{for} \quad W < W_{0_2} \\ W_{0_3} - (W_{0_3} - W_{0_2}) \exp(\mu_2 Y) & \text{else} \end{cases} \tag{33}$$

where

$$\begin{aligned} \mu_1 &= -\frac{\Theta}{2} + \sqrt{\left(\frac{\Theta}{2}\right)^2 + m_1} \\ \mu_2 &= -\frac{\Theta}{2} - \sqrt{\left(\frac{\Theta}{2}\right)^2 + m_3}\,. \end{aligned} \tag{34}$$

This result is obtained by connecting two solutions for linear equations where W is greater or less than W_{0_2} at the threshold boundary, $W = W_{0_2}$.

Scott ([20, p. 104] refers to work on neuristor research in the 1960s where for the model (31) , (32) the traveling-wave speed is given by the expression (translated in our notation)

$$\Theta = \frac{m_1 W_{0_2}^2 - m_3 (W_{0_3} - W_{0_2})^2}{\sqrt{(m_1 W_{0_2} + m_3 (W_{0_3} - W_{0_2}))\,(W_{0_3} - W_{0_2}) W_{0_2} W_{0_3}}}\,. \tag{35}$$

If $m_1 = m_3 = m$, we get

$$\Theta = (2W_{0_2} - W_{0_3}) \sqrt{\frac{m}{(W_{0_3} - W_{0_2}) W_{0_2}}}\,, \tag{36}$$

an expression already given in [21].

7. IMPACT OF GEOMETRIC NONUNIFORMITY ON THE PROPERTIES OF THE ACTION POTENTIAL

The results obtained so far can be used to evaluate the impact of geometric nonuniformity on the properties of the action potential. We remember that the time constant as defined in equations (12) yields – via (6) – a constant both in the domain and the range,

$$t(T) = \tau \cdot t = \frac{C_m}{G_m} \cdot t. \tag{37}$$

Thus a given duration and thus frequency of impulses in the range will not change in the domain.

In contrast, space variables transform back from range into domain by

$$x(X) = \int \lambda(X) \mathrm{d}X = \frac{1}{2\sqrt{R_i G_m}} \int \sqrt{D(X)} \mathrm{d}X, \tag{38}$$

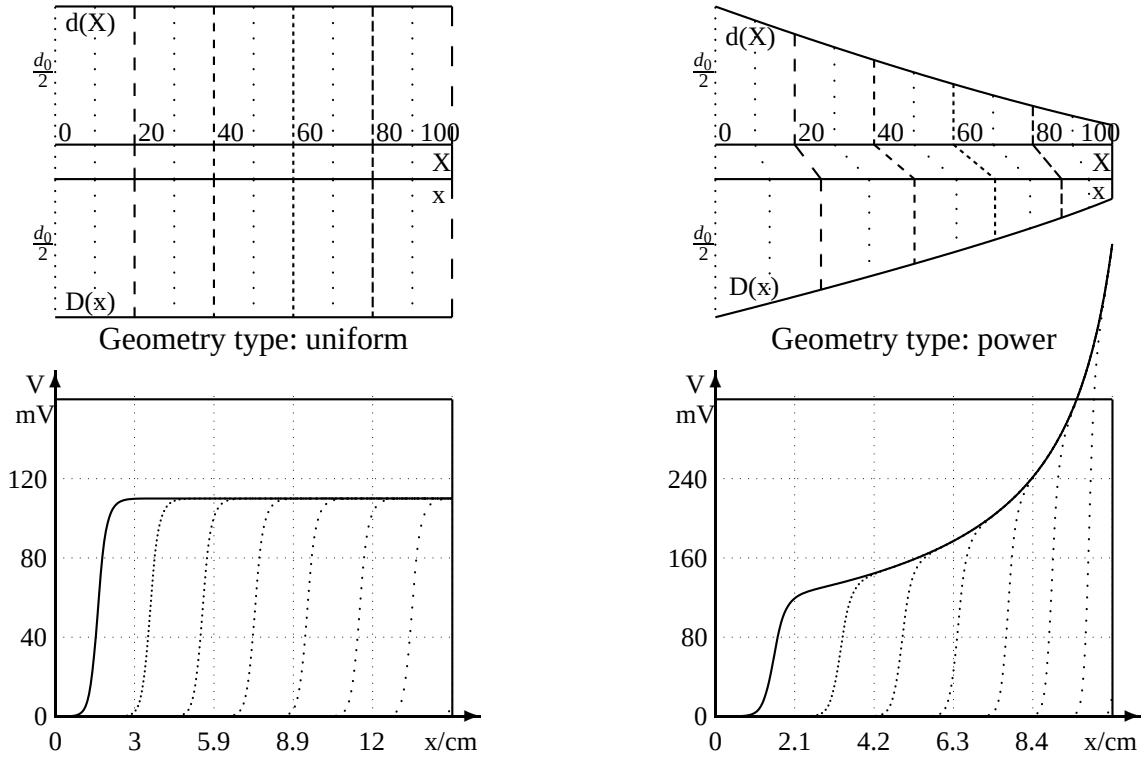

FIGURE 4. Propagation of traveling fronts along axons of the geometry types presented in Tables 1 and 3. In the subfigures, the axon diameter functions $d(x)$ and $D(X)$ in the domain and range are displayed (top), and below snapshots of traveling fronts moving leftwards are presented.

i.e., distances of equal length in the image space have in general different lengths in the domain. This is also true for potential values which transform space-dependent.
A potential of amplitude W in the range yields in the domain a potential V depending on the cable diameter:

$$V = \sqrt[4]{\frac{4R_i}{\pi^2 G_m}} D(X)^{-3/4} W. \tag{39}$$

Traveling front solutions of (constant) speed Θ in the range yield excitation fronts in the domain which propagate with space-dependent speed Θ_x (Figure 4). Using Eqs. (37) and (38), we obtain

$$\Theta_x = \frac{\mathrm{d}x}{\mathrm{d}t} = \frac{\lambda}{\tau}\Theta = \frac{\Theta}{2C_m}\sqrt{\frac{G_m}{R_i} d(x)}. \tag{40}$$

In Figure 4, the propagation of traveling fronts along axon cables obeying the diameter functions given in Tables 1 or 3, respectively, is presented.

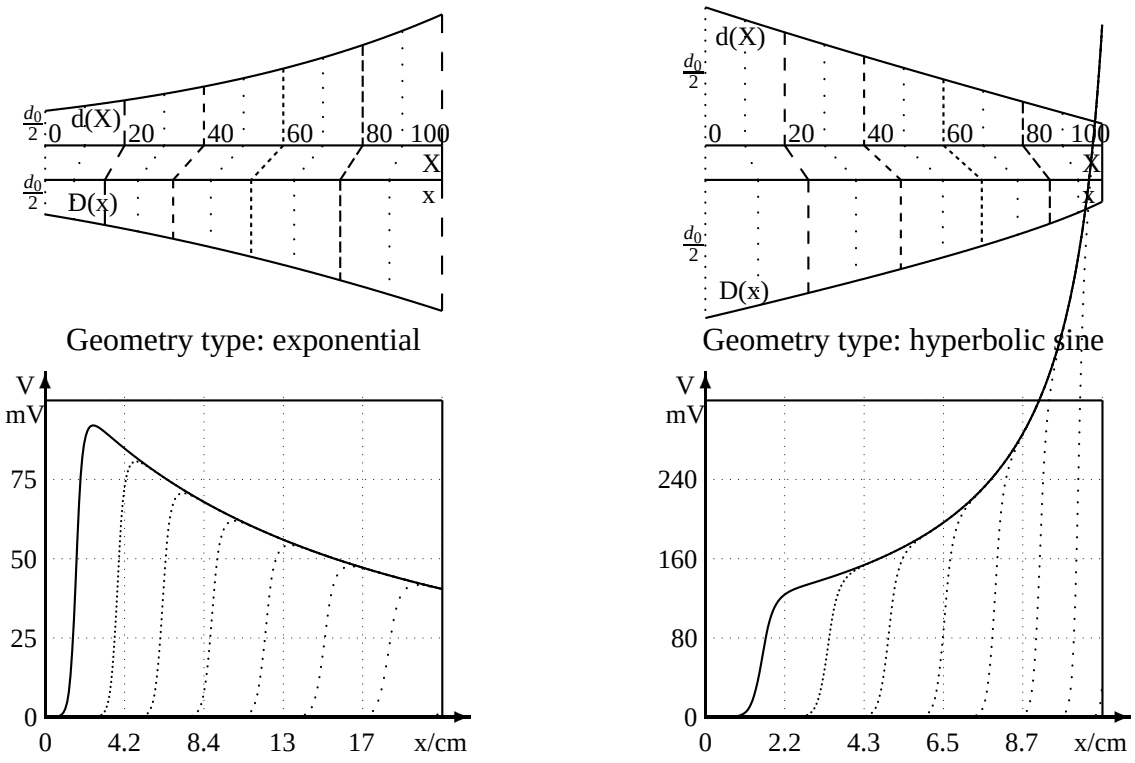

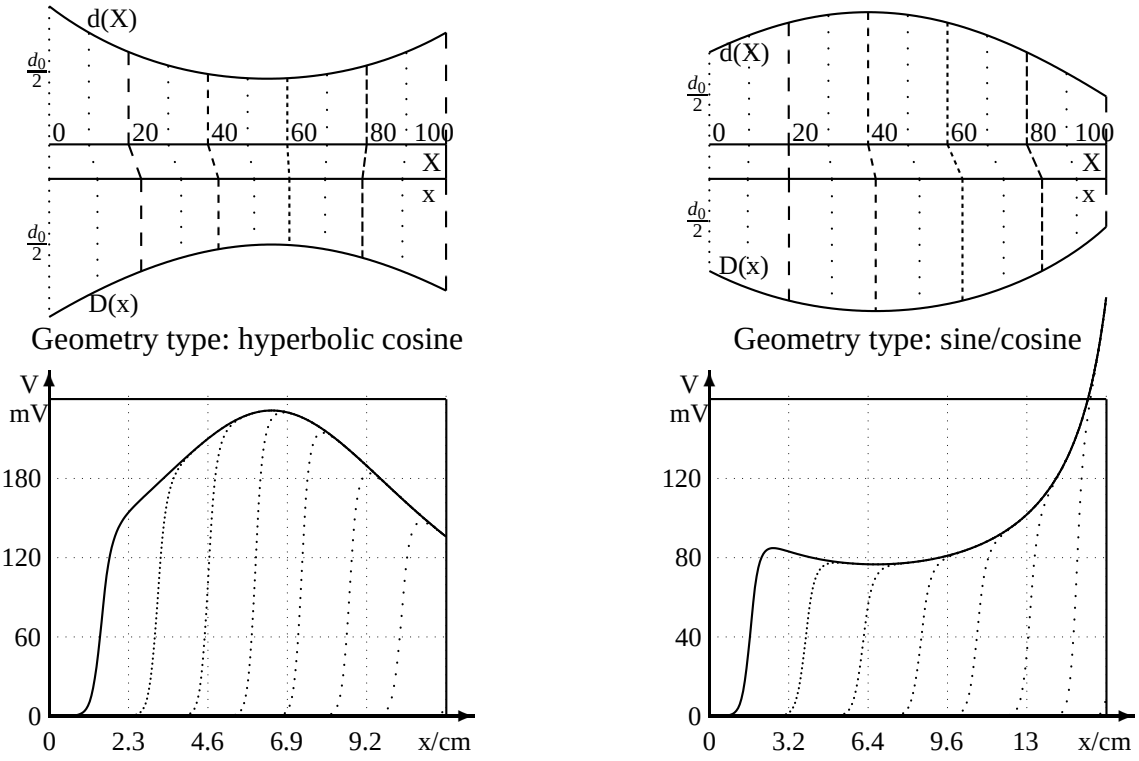

FIGURE 4. (continued).

To summarize, we can state the following conclusions on action potentials propagating along axons of the nonuniform geometry types presented in Tables 1 or 3, respectively:

If the diameter of the axon in the domain widens,

- the speed of the action potential front increases, see (40) and Figure 4,
- the length of the excited axon region increases, see (38) and Figure 4,
- the spike height decreases, see (39) and Figure 4, and
- the spike duration and frequency remain unchanged, see (37).

The method presented in this paper has been also applied to the problem of reducing a dendritic tree with active membrane to an equivalent cable [2]. In that paper, we have stated in a short note that for the piecewise linear FHN model (30),(31) traveling wave solutions can be analytically derived. We will present this case in detail in a forthcoming paper.

REFERENCES

1. A. Schierwagen, *Prog. Brain Res.* **102**, 151–167 (1994).
2. M. Ohme, and A. Schierwagen, *Biol. Cybern.* **78**, 227–243 (1998).
3. G. M. Shepherd, ed., *The Synaptic Organization of the Brain*, Oxford University Press, New York, 1998.
4. G. Stuart, N. Spruston, and M. Häusser, eds., *Dendrites*, Oxford University Press, Oxford, 1999.
5. J. P. Pawelussen, *J. Math. Biology* **15**,151–171 (1982).
6. A. C. Scott, *Rev. Mod. Phys.* **47**, 487–533 (1975).
7. R. FitzHugh: "Mathematical models of excitation and propagation in nerve", in *Biological Engineering*, edited by H. P. Schwan, McGraw-Hill, New York, 1969, pp. 1–85.
8. J. Nagumo, S. Arimoto, and S. Yoshizawa, *Proc. IRE* **50**, 2061–2070 (1962).
9. S. S. Goldstein, and W. Rall, *Biophys. J.* **14**, 731–757 (1974).
10. A. L. Hodgkin, and A. F. Huxley, *J. Physiol. (Lond.)* **117**, 500–544 (1952).
11. J. J. Kelly, and M. S. Ghausi, *IEEE Trans. Circuit Theory* **CT-12**, 554–558 (1965).
12. A. Schierwagen, *J. theor. Biol.* **141**, 159–179 (1989).
13. M. Ohme, *Modellierung der neuronalen Signalverarbeitung mittels kontinuierlicher Kabelmodelle*, Dissertation, Universität Leipzig, Fakultät für Mathematik und Informatik, 1995.
14. P. J. Hunter, P. A. McNaughton, and D. Noble: emphProg. Biophys. Molec. Biol. **30**, 99–144 (1975).
15. S. G. Waxman, J. D. Kocsis, and P. K. Stys, eds., *The Axon. Structure, Function and Pathophysiology.* Oxford University Press, Oxford, 1995.
16. A. Rabinovitch, I. Aviram, N. Gulko, E. Ovsyscher, *J. theor. Biol.* **196**, 141–154, 1999.
17. R. FitzHugh, *J. theor. Biol.* **40**, 517–541 (1973).
18. J. Rinzel, and D. Terman, *SIAM J. Appl. Math.* **42**, 1111–1136 (1982).
19. A. Schierwagen, "Traveling wave solutions of a simple nerve conduction equation for inhomogeneous axons" , in *Nonlinear Waves in Excitable Media*, edited by A. V. Holden, M. Markus, and H. Othmer, Manchester University Press, Manchester, 1991, pp. 107–114.
20. A. Scott, *Neuroscience: A Mathematical Primer*, Springer-Verlag, New York, 2002.
21. J. Rinzel and J. B. Keller, *Biophys. J.* **13**, 1313–1337 (1973).